2021 23rd International Conference on Process Control (PC)
June 1–4, 2021, Štrbské Pleso, Slovakia

Design of an MPC based attitude control system for a CubeSat nanosatellite

Jokhongir Mamarasulov[1,2], Juraj Holaza[2] and Martin Gulan[1]
[1]Institute of Automation, Measurement and Applied Informatics,
Faculty of Mechanical Engineering, Slovak University of Technology in Bratislava
Námestie slobody 17, 812 31 Bratislava, Slovakia, E-mail: jokhongir.mamarasulov@stuba.sk
[2]Honeywell International, Tuřanka 100, 627 00 Brno, Czech Republic

2021 23rd International Conference on Process Control (PC) | 978-1-6654-0330-6/20/$31.00 ©2021 IEEE | DOI: 10.1109/PC52310.2021.9447494

***Abstract*—This paper presents the design of model predictive control (MPC) for a linear time-variant model of a CubeSat nanosatellite. The MPC controller is derived from the formulation of a linear-quadratic regulator (LQR) problem for finding a periodic gain evaluated at each sampling instant. The obtained parameters are subsequently used to formulate the MPC problem. The control law is implemented within a complex simulation environment for attitude determination and control system, which combines spacecraft dynamics and environmental models. We also use the extended Kalman filter to address the sensor fusion problem and to eliminate state estimation errors. Objective of the controller is to track a set of state references corresponding to a predefined observation trajectory. Finally, control performance is numerically demonstrated and compared with LQR.**

I. Introduction

Space exploration has played a significant role in our lives since the beginning of the space era. The satellites back in the 20th century were large and volumetric. The effort to reduce the costs influenced the demand for designing a new class of so-called nanosatellites, also referred to as CubeSats. The standard unit (1U) represents a cube structure with the dimensions of $10 \times 10 \times 10\,\mathrm{cm}^3$ and weight up to $1.33\,\mathrm{kg}$. The 1U CubeSat can be designed as a standalone satellite or merged to build a bigger spacecraft. A distinctive feature of CubeSats from other satellites is that nanosatellites are classified based only on their mass. The evolution of CubeSats since the first launch was briefly discussed in [1]. These satellites have become a significant replacement for bulky and expensive spacecrafts. They are used for various scientific and commercial missions, such as telecommunications, Geo Positioning System (GPS), Internet of Things (IoT); Nanosatellites are even expected to reach the nearest star system Alpha Centauri within the Breakthrough Starshot project [2].

Immediately after the release from a launch pod, the angular velocity of the satellite increases—we say that the satellite tumbles. Another source of rotation is the perturbation caused by ambient noise and environmental models. If these effects act on the spacecraft in a non-periodic way, they can boost its kinetic energy. Control performance requirements may vary from simple radio communication to complex terrain mapping or outer space observations. Many control approaches can be used for attitude control, from basic detumbling, conventional or popular adaptive PID controllers, to complex optimization-based algorithms such as MPC. Most satellite missions use simple B-dot control law for magnetic detumbling if reference tracking is not required. The B-dot law for attitude control was first proposed by Stickler [3]. On the other hand, to fulfill the reference tracking requirements, LQR has recently become more popular thanks to its acceptable computational demands and implementation effort.

This work intends to derive an advanced control algorithm capable of tracking a pre-set reference with a better control performance than the traditionally used controllers, and to inherently account for input constraints imposed by the hardware. Another motivation stems from the initiated cooperation with the Needronix company focused on development of attitude determination and control system (ADCS) for CubeSats. The objective is thus to implement a control strategy to stabilize the satellite as accurately as possible. The most convenient way to accomplish this is to exploit the features of MPC.

MPC is a well-known modern control strategy which has emerged from a genuine symbiosis of feedback control theory and numerical optimization that formulates control engineering objectives in terms of constrained optimization problems, generally leading to improved control performance as well as reduced tuning effort. The main challenge is to certificate the complexity of the underlying algorithm and to find a suitable and reliable optimization solver. This prevents the use of MPC in a wide range of industrial applications. Consequently, it is utilized as a backup algorithm for existing control strategies instead. For example, in [4] the authors introduce a linear time-varying model predictive control of the under-actuated satellite using magnetic coils subject to the dipole moment constraints for nadir and inertial pointing. Work of [5] is dedicated to the design of an advanced on-board fault detection, isolation and recovery (FDIR) algorithm aimed at obtaining the optimal recovery solution while employing MPC for attitude control. The study in [6] investigates the feasibility of achieving 3-axis stabilization of an asymmetric spacecraft with loss of control in one axis using a tube-based MPC algorithm.

In this paper we introduce a stabilizing linear MPC strategy to the control of a 1U CubeSat, implemented in MATLAB. Input constraints imposed by physical limits of the actua-

*The authors gratefully acknowledge the contribution of the Slovak Research and Development Agency under the contract APVV-18-0023.

tors are adopted from the technical description of the first Slovak satellite, designated skCube. The main objective of the proposed controller is to provide a continuous parallax mapping of the terrain by subsequent following of a predefined circular trajectory. Control performance of the proposed MPC controller is demonstrated and numerically compared with the performance of nominal LQR.

II. System equations

When dealing with the analysis of the spacecraft dynamics, it is necessary to define reference coordinate systems to effectively express the orientation of different objects and their relations to each other. Reference coordinate systems or frames used in this work are a control frame, an orbit frame and an Earth frame. The illustration of the introduced frames is represented in Fig. 1. Reference frame fixed to the spacecraft, the so-called satellite control frame $\mathrm{S_c}$, is a right orthogonal coordinate system based on the principal axes of the spacecraft with the origin in the center of mass. The frame is constructed concerning the position of the measurement sensors, and intuitively it is used to describe the orientation of the attitude control system. Second, the right orthogonal coordinate system is the orbit coordinate frame, $\mathrm{S_o}$ define the roll angle around x-axis denoted by the satellite motion across the orbit, yaw angle around y-axis pointing at the zenith and pitch angle around z-axis, which points in the orbital plane normal direction. The orbit coordinate frame is used as a reference for the attitude control system. Finally, the Earth coordinate frame, $\mathrm{S_i}$ is a right orthogonal coordinate system representing the inertial system, where y-axis is parallel to the rotation axis of the Earth, x-axis is parallel to the equator, and z-axis is formed by the vector product of the x and y axes. The satellite control frame coincides with the orbit frame during the nadir pointing stabilization phase.

A. Attitude dynamics

The attitude dynamics is derived from the equations of motion for a rigid body. The Euler's law describes the relationship between the time derivative of the angular momentum vector, $\frac{\partial \mathbf{L}}{\partial t}$, and the applied torque, $\boldsymbol{\tau}$. The time derivative of the components of $\mathbf{L}$ is considered with respect to spacecraft-fixed axes because of the convenience of expressing the moment of inertia tensor in this way. The fundamental equation of rigid body dynamics in $\mathrm{S_c}$ respective to the inertial reference frame, $\mathrm{S_i}$, can be formulated as:

$$\boldsymbol{\tau} = \frac{\partial \mathbf{L}}{\partial t} = \mathbf{I}_\mathrm{b}\boldsymbol{\omega} + \boldsymbol{\omega} \times \mathbf{I}_\mathrm{b}\boldsymbol{\omega}, \tag{1}$$

where $\boldsymbol{\tau} \in \mathbb{R}^3$ represents the torque vector acting on the body and consists of applied control torque, $\boldsymbol{\tau}_\mathrm{c}$, and perturbation torque, $\boldsymbol{\tau}_\mathrm{p}$, caused by external effects, such as aerodynamic torque, magnetic residual torques or gravity gradient torque and $\boldsymbol{\omega} \in \mathbb{R}^3$ denotes angular velocity vector. The vector product can be expressed as a $\mathbb{R}^{3\times3}$ skew-symmetric matrix. $\mathbf{I}_\mathrm{b} \in \mathbb{R}^{3\times3}$ is the body moment of inertia tensor, which is a real, symmetric matrix. Hence it has real eigenvalues and orthogonal vectors, which satisfies the sufficient condition for the $\mathrm{S_b}$ frame to be placed in such way that moment of inertia tensor becomes a diagonal matrix $\mathbf{I}_\mathrm{b} = \mathrm{diag}(I_x, I_y, I_z)$. By assuming the latter and a uniform mass distribution, the moment of inertia tensor can be expressed using:

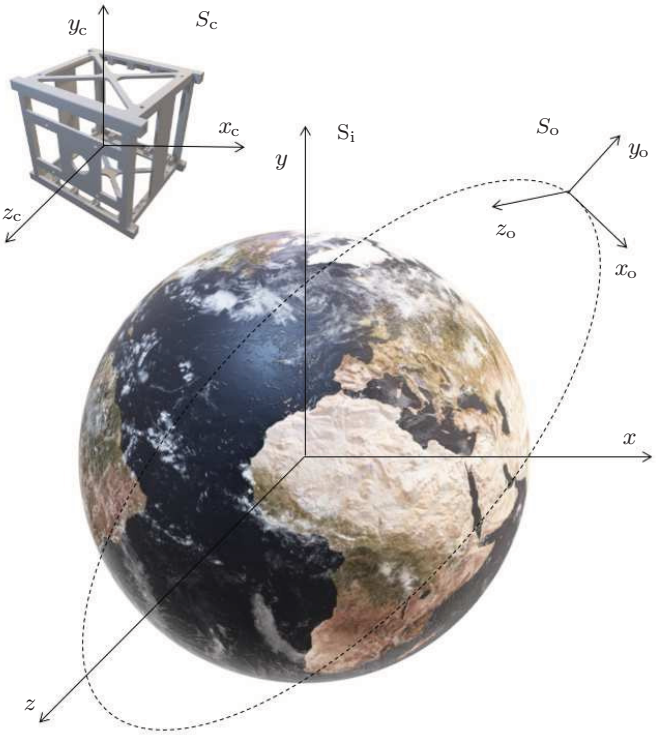

Fig. 1: Illustration of different reference frames.

$$I_x = \frac{m}{12}(b^2 + c^2),$$
$$I_y = \frac{m}{12}(a^2 + c^2),$$
$$I_z = \frac{m}{12}(a^2 + b^2),$$

where m denotes the total mass and a, b, c dimensions of the spacecraft, respectively. Additionally, it is important to note that the impact of the gravity gradient torque on the satellite in (1) is negligible, because the objective of the simulation study is a symmetric cube.

B. Relative kinematics

The spacecraft's relative kinematics is a collection of first-order differential equations that describe the time variation of respective attitude parameters. These parameters are used to express the spacecraft's position in orbit relative to $\mathrm{S_o}$. Various options used for this purpose are discussed in detail in [7]. One of the most common methods is to describe any rotation by a set of three orthonormal angles. This method is known as Euler's angles. The strategic disadvantage of such parameters is the occurrence of singularities. Here, we assume quaternions for attitude parametrization. Although they lack an intuitive physical meaning, they impose no singularities, and such a

representation is well suited for integrating the attitude of the spacecraft over time. The kinematic differential equations using the quaternions can be formulated as follows:

$$\dot{\mathbf{q}} = \frac{1}{2}\begin{bmatrix} 0 & \omega_3 & -\omega_2 & \omega_1 \\ -\omega_3 & 0 & \omega_1 & \omega_2 \\ \omega_2 & -\omega_1 & 0 & \omega_3 \\ -\omega_1 & -\omega_2 & -\omega_3 & 0 \end{bmatrix} \mathbf{q}, \tag{2}$$

where $\mathbf{q} \in \mathbb{R}^4$ represents the unit quaternion, which consists of the real part, η, and the three-dimensional imaginary part, $[q_1, q_2, q_3]^{\mathrm{T}}$, and $\boldsymbol{\omega}$ denotes the body's angular velocity vector from (1).

C. Nonlinear model

Attitude dynamics and relative kinematics presented above can be merged into a system of nonlinear equations that describe the motion and position of the spacecraft. After some rearrangement and mathematical manipulation we obtain:

$$\dot{\boldsymbol{\omega}} = \mathbf{I}_{\mathrm{b}}^{-1}(-\mathrm{S}(\boldsymbol{\omega})\mathbf{I}_{\mathrm{b}}\boldsymbol{\omega} + \boldsymbol{\tau}_{\mathrm{c}} + \boldsymbol{\tau}_{\mathrm{p}}), \tag{3a}$$

$$\dot{\mathbf{q}} = \frac{1}{2}\mathbf{W}(\boldsymbol{\omega})\mathbf{q}, \tag{3b}$$

where $\mathrm{S}(\cdot)$ denotes an operator of a skew-symmetric matrix. Note that the magnitude of the input control torque $\boldsymbol{\tau}_{\mathrm{c}}$ is about a thousand times greater than the magnitude of perturbation torque $\boldsymbol{\tau}_{\mathrm{p}}$.

The nonlinearity in (1) occurs due to the vector product of the angular velocity state vectors. The additional nonlinearity in (2) stems from the product of the angular velocity rotation matrix and the unit quaternion. It is difficult to control nonlinear systems because of the strong dependency of respective system variables. In order to linearize the system equations, we need to reformulate (3) into a representative form. By substituting the state vector $\mathbf{x} = [x_1, \ldots, x_7]^{\mathrm{T}} = [\eta, q_1, q_2, q_3, w_1, w_2, w_3]^{\mathrm{T}}$ into (3) and assuming that both attitude and angular velocity are measured, we obtain the following continuous nonlinear state-space model:

$$\begin{bmatrix} \dot{x}_1 \\ \dot{x}_2 \\ \dot{x}_3 \\ \dot{x}_4 \\ \dot{x}_5 \\ \dot{x}_6 \\ \dot{x}_7 \end{bmatrix} = \begin{bmatrix} -\frac{x_2x_1}{2} - \frac{x_3x_2}{2} - \frac{x_4x_3}{2} \\ \frac{x_1}{2} + \frac{x_3}{2} - \frac{x_4x_2}{2} \\ \frac{x_1x_2}{2} - \frac{x_2x_3}{2} + \frac{x_4x_1}{2} \\ \frac{x_1x_3}{2} + \frac{x_2x_2}{2} - \frac{x_3x_1}{2} \\ \frac{u_1 + I_y x_2 x_3 - I_z x_2 x_3}{I_x} \\ \frac{u_2 - I_x x_1 x_3 + I_z x_1 x_3}{I_y} \\ \frac{u_3 + I_x x_1 x_2 - I_y x_1 x_2}{I_z} \end{bmatrix}, \quad \begin{bmatrix} y_1 \\ y_2 \\ y_3 \\ y_4 \\ y_5 \\ y_6 \\ y_7 \end{bmatrix} = \begin{bmatrix} x_1 \\ x_2 \\ x_3 \\ x_4 \\ x_5 \\ x_6 \\ x_7 \end{bmatrix}. \tag{4}$$

Note that the MIMO model (4) has three inputs $\mathbf{u} = [u_1, u_2, u_3]^{\mathrm{T}}$ given by the total torque generated in the three corresponding axes.

D. Linearized model

In order to apply linear system theory and control law, we approximate model (4) using the first-order Taylor expansion around the desired operating point given by $[\breve{\mathbf{x}}^{\mathrm{T}}, \breve{\mathbf{u}}^{\mathrm{T}}] = [x_1, \ldots, x_7, 0, 0, 0]$, meaning the linearized model is varying depending on the state configuration. The nominal linearized time-variant state-space model is then given as follows:

$$\Delta\dot{\mathbf{x}}(t) = \mathbf{A}_{\mathrm{c}}(t)\Delta\mathbf{x}(t) + \mathbf{B}_{\mathrm{c}}\Delta\mathbf{u}(t), \tag{5a}$$

$$\Delta\mathbf{y}(t) = \mathbf{C}_{\mathrm{c}}\Delta\mathbf{x}(t), \tag{5b}$$

where $\mathbf{x}(t)$ and $\mathbf{y}(t)$ are the state vectors, $\Delta\mathbf{x} = \mathbf{x} - \breve{\mathbf{x}}$, $\Delta\mathbf{u} = \mathbf{u} - \breve{\mathbf{u}}$ and $\Delta\mathbf{y} = \mathbf{y} - \mathbf{h}(\breve{\mathbf{x}}, \breve{\mathbf{u}})$ represent the deviations of variables from respective operating points. An additional attention has to be drawn to the state transition matrix, $\mathbf{A}_{\mathrm{c}}(t)$, which is a function of time. In the case of varying state matrix, the linear approximation has to be performed separately for each particular state configuration in order to parametrize the control law.

Since the on-board sensors provide digital outputs, the linear system (5) has to be further discretized for the state estimation purposes. Discretizing the derived model via zero-order hold reconstruction with a sampling period T, which represents an inverse of the maximum frequency of the continuous-time signal, yields the linear discrete-time state-space model denoted as:

$$\mathbf{x}(k+1) = \mathbf{A}(k)\mathbf{x}(k) + \mathbf{B}\mathbf{u}(k), \tag{6a}$$

$$\mathbf{y}(k) = \mathbf{C}\mathbf{x}(k), \tag{6b}$$

where the $\Delta(\cdot)$ notation was omitted in order to simplify further explanations.

E. State estimation

The navigation satellites operating in the orbit are subject to external forces that generate orbital irregularities or perturbations, namely the noise of attitude sensors and perturbation torque arising from environmental models. The more attitude sensors are used in the satellite's ADCS system, the greater error they produce. Moreover, many contrasting types of sensors provide different information that has to be fused for further processing. These perturbations must be accurately predicted to obtain an estimate of the system state that enters the MPC problem. In this work, we used the extended Kalman filter (EKF) [8] for this purpose.

The linearization must be a satisfying approximation of the nonlinear model in terms of all uncertainties associated with the state estimate in order to obtain a reliable state prediction. EKF assumes the following discrete-time model [8]:

$$\mathbf{x}_{k+1} = \mathbf{f}(\mathbf{x}_k) + \mathbf{w}_k, \tag{7a}$$

$$\mathbf{y}_k = \mathbf{h}(\mathbf{x}_k) + \mathbf{v}_k, \tag{7b}$$

where $\mathbf{f}(x)$ is the nonlinear discrete function derived from (3) using Euler integration, $\mathbf{h}(k)$, is an observation function represented by a quaternion matrix arising from simple rotations around two body axes in the centre of the satellite. Next, $\mathbf{w}(k)$ and $\mathbf{v}(k)$ denote additive zero-mean multivariate Gaussian noises represented by a function of perturbation torque and white independent random noise with covariance matrices $\mathbf{Q}_{\mathrm{f}}$ and $\mathbf{R}_{\mathrm{f}}$, respectively.

The on-board attitude sensors provide information about the current orientation of the satellite with respect to the inertial frame. The gathered information is then fused and processed as a three-dimensional input vector by the filter. EKF is initialized

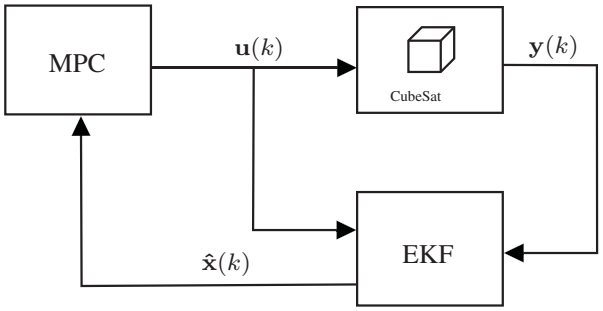

Fig. 2: Simplified block scheme of the proposed MPC based attitude control system.

with a random Gaussian vector and after a short period the state error converges to zero.

III. Controller design

In this section we present control algorithms based on the derived system equations. After processing the input position vector, the EKF outputs the state estimate that is further fed to the MPC controller, as shown in Fig. 2. The controller gathers the information about the state of the satellite to calculate the optimal control action to be applied to the spacecraft model.

A. Linear quadratic control

The LQR for spacecrafts using magnetorquers was well-documented by [9]. This problem can be stated as obtaining the control input that minimizes the following cost function:

$$J_k = \mathbf{x}_N^{\mathrm{T}} \mathbf{P}_k \mathbf{x}_N + \sum_{k=0}^{N-1} (\mathbf{x}_k^{\mathrm{T}} \mathbf{Q} \mathbf{x}_k + \mathbf{u}_k^{\mathrm{T}} \mathbf{R} \mathbf{u}_k), \tag{8}$$

where the state cost and terminal state weighting matrices, $\mathbf{Q}$ and $\mathbf{P}(k)$, are positive semi-definite and input cost matrix $\mathbf{R}$ is positive definite. The solution of (6) takes form of the following feedback control law:

$$\mathbf{u}(k) = -\mathbf{K}(k)\mathbf{x}(k), \tag{9}$$

where the gain $\mathbf{K}(k)$ corresponds to the solution to the optimal control problem at a given sampling time and is obtained by solving the discrete algebraic Riccati equation (DARE).

System (6) is time-varying with a periodic state transition matrix $\mathbf{A}(k)$ of period T and a constant input matrix $\mathbf{B}$. Once the DARE equation is solved, we can evaluate the input vector, $\mathbf{u}(k)$ per (9). When the obtained input exceeds the constraint limit, it is subjected to saturation.

B. Model predictive control

The MPC problem for the satellite attitude control can be formulated as follows:

$$\min_{\mathbf{U}} \quad \mathbf{x}_N^{\mathrm{T}} \mathbf{P}_k \mathbf{x}_N + \sum_{k=0}^{N-1} (\mathbf{x}_k^{\mathrm{T}} \mathbf{Q} \mathbf{x}_k + \mathbf{u}_k^{\mathrm{T}} \mathbf{R} \mathbf{u}_k) \tag{10a}$$

$$\text{s.t.} \quad \mathbf{x}_{k+1} = \mathbf{A}_k \mathbf{x}_k + \mathbf{B}\mathbf{u}_k, \; k = 1, \ldots, N-1, \tag{10b}$$

$$\mathbf{x}_0 = \mathbf{x}(k), \tag{10c}$$

$$\boldsymbol{\tau}_{\min} \leq \mathbf{u}_k \leq \boldsymbol{\tau}_{\max}, \tag{10d}$$

TABLE I: Simulation model parameters.

Parameter	Symbol	Value	Unit
Total mass	m	1.056	kg
Inertia matrix	$\mathbf{I}_{\mathrm{b}}$	$\begin{bmatrix} 319 & 0 & 0 \\ 0 & 420 & 0 \\ 0 & 0 & 521 \end{bmatrix} \times 10^{-6}$	$\mathrm{kg\,m^2}$
Initial rate	$\boldsymbol{\omega}_0$	$[0.05, -0.05, 0.05]^{\mathrm{T}}$	rad
Sampling period	T	0.1	s
Perturbation torque rate	$\boldsymbol{\tau}_{\mathrm{p}}$	9.1×10^{-8}	$\mathrm{N\,m}$
Measurement noise rate	$\mathbf{v}_{\mathrm{m}}$	2	$^\circ$
Initial attitude	$\mathbf{q}_0$	$[0, 0, 0, 1]^{\mathrm{T}}$	–

where $\mathbf{x}_k \in \mathbb{R}^7$ and $\mathbf{u}_k \in \mathbb{R}^3$ denote state and control input predictions over a finite prediction horizon $N = 10$ at time instant k, initialized by the current state $\mathbf{x}_0 = \mathbf{x}(k)$. Further, $\mathbf{Q}$ and $\mathbf{R}$ are penalization matrices introduced in (8), and $\mathbf{P}(k) \succeq \mathbf{0}$ is the terminal penalty, which can be obtained by solving discrete Lyapunov equation. $\mathbf{U}^\star(k) = [\mathbf{u}_0^{\star\mathrm{T}}, \ldots, \mathbf{u}_{N-1}^{\star\mathrm{T}}]$ denotes the resulting sequence of optimal control moves. The receding horizon control policy is enforced via $\mathbf{u}^\star(k) = [\mathbf{I}, \mathbf{0}, \ldots, \mathbf{0}]\mathbf{U}^\star(k)$, where $\mathbf{I}$ and $\mathbf{0}$ denote identity and zero matrices, respectively.

The MPC control algorithm can be summarized in the following consecutive steps:

1) Obtain the estimated state vector $\hat{\mathbf{x}}(k)$ from EKF.
2) Feed the state vector $\mathbf{x}(k)$ into matrix $\mathbf{A}(k)$ from (6).
3) Obtain the system gain $\mathbf{K}(k)$ to find the terminal penalty $\mathbf{P}(k)$ by solving discrete Lyapunov equation.
4) Construct Hessian and Gradient matrices and feed them to the solver along with the state vector $\mathbf{x}(k)$.
5) Evaluate input vector $\mathbf{u}(k)$ by solving (10) and apply it to the system (6).
6) Repeat the procedure from step (1) at next sample time.

IV. Simulation results

This section presents the performance of EKF (7) state estimator along with the simulation results of the tested LQR (9) and MPC (10) controllers. Several essential parameters of the satellite must be chosen to support a continual run of the simulation and to test the designed controllers thoroughly. Some of the parameters, such as initial rate, $\boldsymbol{\omega}_0$, and perturbation torque rate, $\boldsymbol{\tau}_{\mathrm{p}}$, are the best guesses and values, suggested by [10]. CubeSat is simulated in a circular orbit assuming an inclination of 90° at $500\,\mathrm{km}$ altitude with the initial state $\mathbf{x}_0 = [\mathbf{q}_0, \boldsymbol{\omega}_0]^{\mathrm{T}}$. An overview of the simulation setup can be found in Table I. The executive task of the controller is to maintain the exclusive domain of various orientations. The observation trajectory is formed by drawing a circle with a radius of π in the nadir-pointing plane, creating a set of 42 rotations around the center. Note that initial attitude here represents both the first and last reference orientation and the reference vector corresponds to $\mathbf{x}_{\mathrm{ref}} = [\mathbf{q}_{\mathrm{ref}}^i, 0, 0, 0]^{\mathrm{T}}$, where $i = 1, \ldots, 42$. The initial assumption of geostationary mission comprehends the ability of the satellite to conduct the on-board experiment during the interval of 10 seconds while being in the desired orientation. The perturbation torque and the measurement noise were modeled as random functions multiplied by the corresponding rates.

The performance of EKF is represented by attitude and rate errors. First, the quaternion rotational error is defined as $\delta q = \mathbf{q} \bigotimes \mathbf{q}_{\mathrm{ref}^{-1}}$, where $\mathbf{q}_{\mathrm{ref}^{-1}}$ denotes quaternion inverse of the reference quaternion rotation and $\bigotimes$ represents the quaternion product. On the other hand, the rate error, $\delta\omega$, is evaluated based on normalized difference of estimated state and true value of the state. The performance of state estimation for both controllers was nearly identical. Figure 3 depicts the state errors arised during the testing of MPC controller. It can be observed that EKF errors are inadequately high during the initialization phase. Nonetheless, the estimator minimizes the errors after some cycles with a mean attitude rotational error of $1.19°$ and a mean rate error of $0.31\,°/\mathrm{s}$.

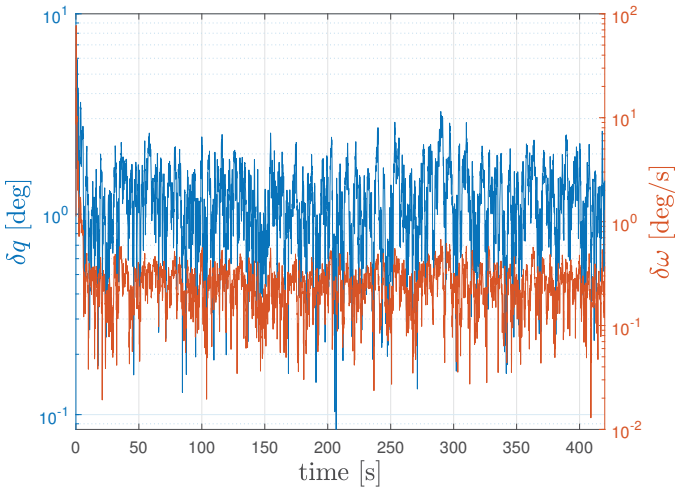

Fig. 3: Attitude and rate errors obtained using EKF.

The varying LQR gain has been calculated by assuiming $\mathbf{R} = \mathbf{I}_3$ and $\mathbf{Q} = \mathrm{diag}(8, 8, 8, 8, 3, 3, 3)$. As mentioned earlier, the underlying quadratic problem (8) of MPC controller is recursively evaluated at each sampling instant utilizing an active-set algorithm implemented in the open-source solver qpOASES [11]. The maximum input torque is defined by the capabilities of the control hardware. For the simulation purposes, maximum torque is limited to the torque generated by the magnetic coils of the skCube satellite, $\boldsymbol{\tau}_{\max} = \pm[5, 5, 5]^{\mathrm{T}} \times 10^{-4}\mathrm{Nm}$.

Figures 4 and 5 present the evolution of the system states during the effort of tracking the preset sequence of 42 reference orientations reproducing the Earth mapping task in orbit. Figure 4 represents the attitude quaternion, and Fig. 5 shows the angular velocity profiles. Abrubt changes in angular velocities can cause the vibrations damaging the satellite and reducing its lifespan. The velocity reference in Fig. 5 is a constant vector of zeros since the algorithm intends to detumble the satellite. It can be seen from the state profiles that the performance of the MPC controlled satellite is more smooth in comparison with the performance of LQR. This behavior is given by the nature of the control law (10), where the controller adopts the external perturbations as corrections to the model when subjected to constraints violation. The terminal constraints have eventually not been assumed because of the quaternions' characteristics, which never exceed the interval $[-1, 1]$. The corresponding control input profiles are depicted in Fig. 6, representing the effort exerted by the controllers. One may evidence the more aggressive nature of linear quadratic regulator (LQR), the reason of which stems in inability of LQR to inherently account for the input constraints. Thus, the controller is subjected to a meticulous tuning, so the input is algorithmically saturated when the constraint violation occurs. In real-life applications, the 'amount' of control input may relate to the torque generated by the satellite in orbit. The CubeSat consumes the more energy, the more torque it generates, and actuators are thus exposed to undesirable wear.

Conclusion

This paper presented the design of MPC for a 1U CubeSat. The obtained control input was fed into a complex simulation environment for ADCS, which combined spacecraft dynamics and environmental models. The simulation environment will be further utilized to model the initial hardware package in collaboration with the Needronix company. Although there is no doubt about the superiority of MPC over LQR in terms of constraint handling, the nonlinear nature of rotational dynamics hinders its entire control potential. The next steps will therefore involve design of a nonlinear model predictive control (NMPC) algorithm. The implementation of such control strategy should allow to detumble the satellite instantly and follow the reference regardless of the initial position.

References

[1] A. Poghosyan and A. Golkar, "CubeSat evolution: Analyzing CubeSat capabilities for conducting science missions," *Progress in Aerospace Sciences*, vol. 88, pp. 59–83, 2017.

[2] K. L. Parkin, "The Breakthrough Starshot system model," *Acta Astronautica*, vol. 152, pp. 370–384, 2018.

[3] A. C. Stickler, "A magnetic control system for attitude acquisition," vol. 42. Ihaco, Inc., 1972, pp. 8–16.

[4] J. Kim, Y. Jung, and H. Bang, "Linear time-varying model predictive control of magnetically actuated satellites in elliptic orbits," *Acta Astronautica*, vol. 151, pp. 791–804, 2018.

[5] L. Franchi, L. Feruglio, R. Mozzillo, and S. Corpino, "Model predictive and reallocation problem for cubesat fault recovery and attitude control," *Mechanical Systems and Signal Processing*, vol. 98, pp. 1034–1055, 2018.

[6] M. Mirshams and M. Khosrojerdi, "Attitude control of an underactuated spacecraft using tube-based MPC approach," *Aerospace Science and Technology*, vol. 48, pp. 140–145, 2016.

[7] J. Diebel, "Representing attitude: Euler angles, unit quaternions, and rotation vectors," vol. 35, pp. 7–18, 2006.

[8] M. I. Ribeiro, "Kalman and extended Kalman filters: Concept, derivation and properties." Lisboa, Portugal: Institute for Systems and Robotics, 2004, technical report.

[9] R. Wisniewski, "Satellite attitude control using only electromagnetic actuation," Ph.D. dissertation, 1997.

[10] J.Wertz, *Spacecraft attitude determination and control*. Dordrecht, Holland: D. Reidel, 1978, vol. 877.

[11] H. J. Ferreau, C. Kirches, A. Potschka, H. G. Bock, and M. Diehl, "qpOASES: a parametric active-set algorithm for quadratic programming," *Mathematical Programming Computation*, vol. 6, no. 4, pp. 327–363, 2014.

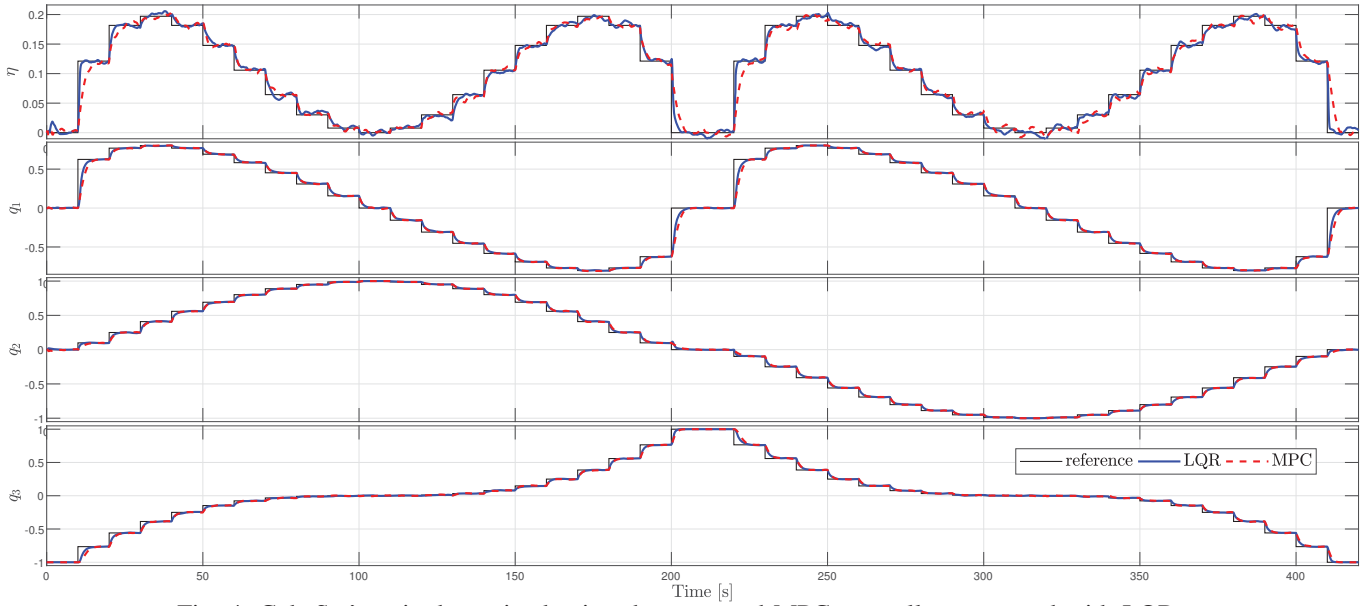

Fig. 4: CubeSat's attitude attained using the proposed MPC controller compared with LQR.

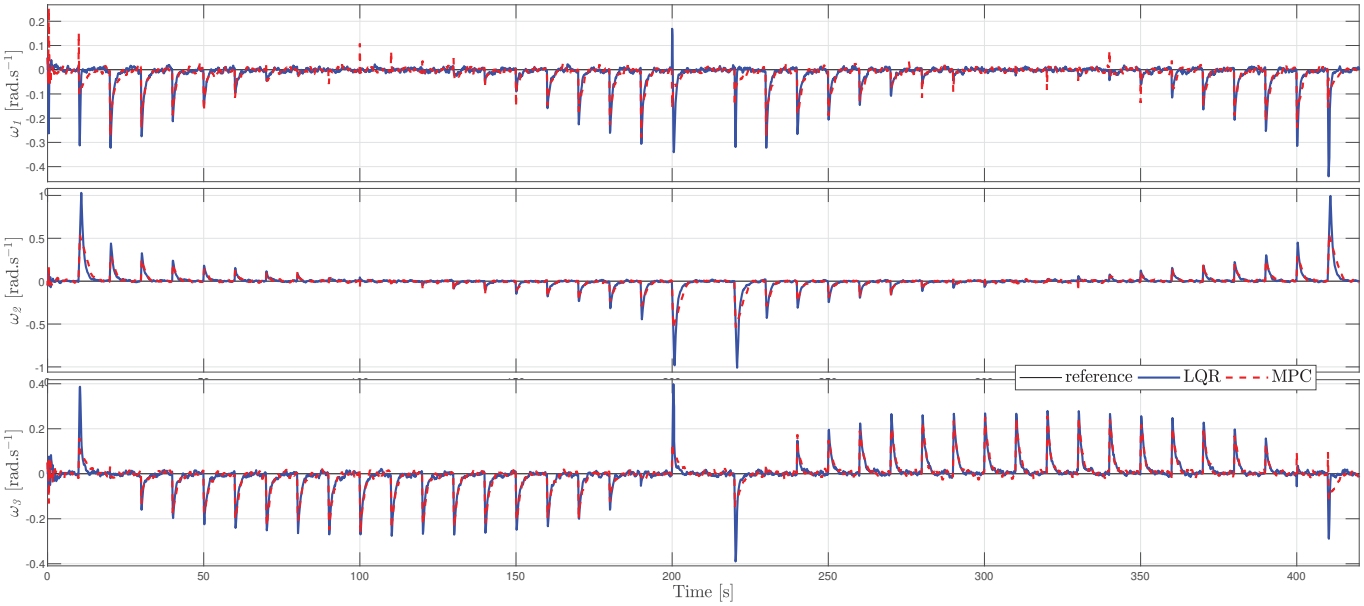

Fig. 5: CubeSat's angular velocity attained using the proposed MPC controller compared with LQR.

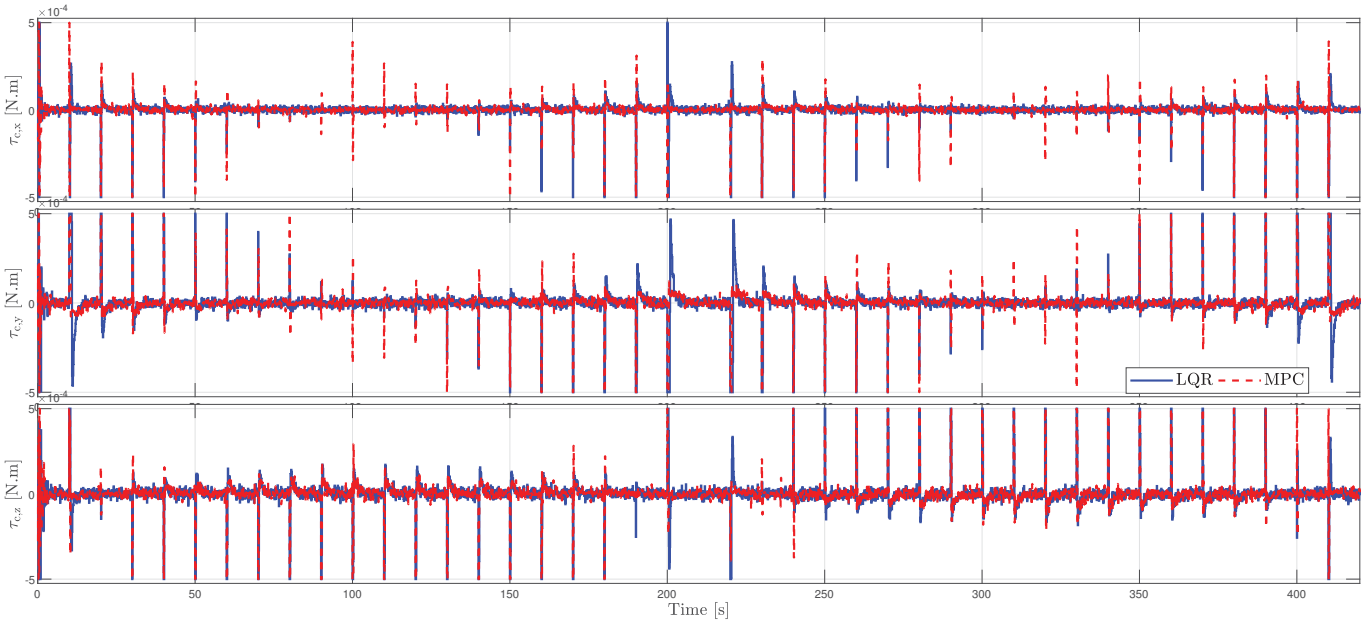

Fig. 6: CubeSat's input torque computed by the proposed MPC controller compared with LQR.